Chromite and chrome spinel occurrences from metacarbonates of the Oetztal–Stubai Complex (northern Tyrol, Austria)

A. MOGESSIE, F. PURTSCHELLER AND R. TESSADRI

Department of Mineralogy and Petrography, University of Innsbruck, A-6020 Innsbruck, Austria

Abstract

Chromite inclusions in uvarovite–chrome garnet, chemically zoned chromite–chrome spinel and chrome spinel–olivine pairs from metacarbonates of the Oetztal–Stubai Complex (northern Tyrol, Austria) are described in terms of their textural occurrences and chemical compositions. Their genetic relationship in relation to the polymetamorphism of the region is discussed.

KEYWORDS: chromite, metacarbonates, Oetztal-Stubai Complex, Austria.

Introduction

EVEN though there is a large literature on chromite occurrences in mafic and ultramafic rocks (Haggerty, 1976), the occurrence of chromite in metacarbonates is rare, and when it occurs, like at Outokumpu (Finland), it is always associated with serpentinites (Eskola, 1933; von Knorring, 1951; von Knorring *et al.*, 1986). In Pollestal, Oetztal–Stubai Complex (northern Tyrol, Eastern Alps), chromite and chrome spinel occur in metacarbonates. The metacarbonates occur as lenses within the central Oetztal amphibolite mass, surrounded by amphibolites and granitic gneisses. In a detailed petrographic study of over 200 samples of metacarbonates and their metabasite inclusions, chromite and chrome spinel have been observed only in three metacarbonates (samples PT-27, PT-166 and PT-179). These samples represent three different textural occurrences of chromite and chrome spinel. They are not typical or representative and are sufficiently out of the ordinary to warrant investigation. In this paper an attempt is made to document and discuss the textural occurrences and compositional variations of the chromite and chrome spinel in light of the polymetamorphic nature of the region.

Geological setting

The Oetztal–Stubai Complex (Eastern Alps) is an overthrusted mass, mainly consisting of a pre-Hercynian rock series, covered by Mesozoic metasedimentary units (Brenner Mesozoics). The principal para-rock types are quartzo-feldspathic biotite gneisses, mica schists, calc-silicates and quartzites. Rocks of magmatic origin include granitic to granodioritic gneisses, amphibolites, peridotites and eclogites (Mogessie *et al.*, 1985). These pre-Hercynian para- and ortho-rocks of the basement are cut by younger post-Hercynian diabase dykes (Purtscheller and Rammlmair, 1982).

In central Oetztal, at the edge of the amphibolite mass, sporadic small layers and lenses of metamorphic carbonate rocks occur, in maximum not thicker than about 50 m. The carbonate rocks have inhomogeneous compositions and complex mineral parageneses due to the polymetamorphic nature of the region (pre-Hercynian, Hercyian and Alpine). The mineral assemblage (carbonate, diopside, forsterite, apatite, humite, tremolite, phlogopite etc.) is post-kinematic and consistent with the amphibolite facies metamorphism of the enclosing rocks. There is no indication of a metasomatic zonation at the contact with the country rock. Inclusions of the surrounding metabasites, eclogites and granites of different size (from mm to several cm) have been found in these metacarbonates. All steps of alteration from the eclogites to amphibolites in the surrounding rocks are also represented among these inclusions (Purtscheller and Sassi, 1975; Mogessie and Purtscheller, 1986; Mogessie *et al.*, 1986).

Analytical methods

Chemical compositions of the chromites, chrome spinels and associated minerals were

Mineralogical Magazine, April 1988, Vol. 52, pp. 229–236

determined with an ARL-SEMQ electron microprobe with four wavelength-dispersive spectrometers at the Institute of Mineralogy and Petrography, University of Innsbruck. An attached energy dispersive system (KEVEX) was used for quick qualitative and semiquantitative analyses. The conditions for wavelength dispersive analyses were 15 kV accelerating voltage, 0.04 μa sample current and 20 sec counting time. As standards natural minerals were used (chromite, spinel, gahnite, tephroite, garnet, kaersutite, jadeite, and orthoclase). The matrix effects were corrected according to Bence and Albee (1968).

Type 1: chromite–uvarovite–chromian minerals–carbonate

One of the metacarbonate samples (PT-27) has dark chromite grains scattered within a garnet that is associated with hornblende, diopside, omphacite, plagioclase and biotite within a carbonate–biotite matrix.

Chromite. Based on a large number of electron microprobe analyses (about 30 points), the chromite was found to be relatively homogeneous and is Cr- and Fe-rich (Cr_2O_3 59–61 wt. %, FeO 27.6–28.2 wt. %; representative avarage analyses are given in Table 1). The amount of ZnO present (2.52 wt. %), compared with those of von Knorring *et al.* (1986) from Outokumpu, implies that this chromite is zincian. The chromite analyses fall on the Fe–Cr-rich edge of the base of the spinel prism (Fig. 4) with a $Cr/(Cr + Al) = 0.84$ and $Mg/(Mg + Fe^{2+}) = 0.10$.

Zoned chrome-garnet (uvarovite). Table 1 shows the analyses of garnet associated with chromite. The amount of Cr_2O_3 in garnet decreases from 12.90 wt. % in GA1 to 4.72 wt. % in GA2 and 2.31 wt. % in GA3. At the same time the

Table 1: Representative electronmicroprobe analyses (sample PT-27) of chromite and associated minerals

	CHR	GA1	GA2	GA3	HBL1*	HBL2	OMPH1*	OMPH2	CPX1*	CPX2	RT1*	RT2
SiO_2	-	37.02	38.21	38.61	39.14	40.82	54.55	55.40	50.38	52.94	n.d.	n.d.
TiO_2	0.61	0.35	0.28	0.13	0.38	0.37	0.30	0.08	0.08	0.08	96.83	98.84
Al_2O_3	7.46	11.49	18.42	20.60	18.34	18.35	10.52	12.83	5.72	5.81	0.06	0.12
Cr_2O_3	59.01	12.90	4.72	2.31	1.04	0.14	2.06	0.03	2.72	0.28	1.52	0.04
Fe_2O_3	0.00	1.87	0.56	0.16	-	-	3.40	0.62	4.05	0.28	-	-
FeO	28.17	7.23	12.92	14.33	13.53	12.15	1.26	1.99	0.19	3.76	0.76	0.71
MnO	0.34	0.31	0.45	0.53	0.20	0.11	0.02	0.06	0.06	0.04	-	0.02
MgO	1.69	1.69	3.57	3.95	9.61	10.63	7.98	8.19	13.31	12.89	0.04	0.06
ZnO	2.52	n.d.	n.d.	n.d.	n.d.	n.d.	n.d.	n.d.	n.d.	n.d.	0.02	0.02
CaO	-	26.56	20.45	19.03	12.31	12.10	12.57	13.18	21.73	21.98	n.d.	n.d.
K_2O	-	-	-	-	1.20	1.60	-	-	0.02	-	n.d.	n.d.
Na_2O	-	-	-	-	2.68	2.25	7.31	7.07	1.83	1.82	n.d.	n.d.
Total	99.80	99.42	99.58	99.65	98.43	98.52	99.97	99.45	100.09	99.88	100.04	99.81
Oxygens	32	24	24	24	23	23	6	6	6	6	4	4
Si	-	5.940	5.953	5.961	5.813	5.978	1.949	1.964	1.844	1.930	-	-
Ti	0.128	0.042	0.033	0.015	0.043	0.041	0.008	0.002	0.002	0.002	1.965	1.987
Al^{IV}	-	0.060	0.047	0.039	2.187	2.023	0.051	0.036	0.156	0.070	-	-
Al^{VI}	2.504	2.113	3.385	3.709	1.023	1.144	0.392	0.500	0.091	0.179	0.002	0.004
Cr	13.288	1.637	0.581	0.282	0.122	0.016	0.058	0.001	0.079	0.008	0.032	0.001
Fe^{3+}	0.000	0.226	0.065	0.019	-	-	0.091	0.017	0.111	0.008	-	-
Fe^{2+}	6.712	0.970	1.684	1.850	1.680	1.488	0.038	0.059	0.006	0.115	0.017	0.016
Mn	0.080	0.042	0.059	0.069	0.025	0.014	0.001	0.002	0.002	0.001	-	0.001
Mg	0.720	0.404	0.829	0.909	2.127	2.320	0.425	0.433	0.726	0.700	0.002	0.002
Zn	0.536	-	-	-	-	-	-	-	-	-	-	-
Ca	-	4.566	3.414	3.148	1.959	1.898	0.481	0.501	0.852	0.858	-	-
K	-	-	-	-	0.227	0.299	-	-	0.001	-	-	-
Na	-	-	-	-	0.772	0.639	0.506	0.486	0.130	0.129	-	-
Total	23.968	16.000	16.000	16.001	15.978	15.860	4.000	4.001	4.000	4.000	2.018	2.011

CHR = chromite inclusion in uvarovite - chrome bearing garnet; GA1 - GA3 = garnets (see also Fig.1);
HBL1,2 = hornblendes; OMPH1,2 = omphacites; CPX1,2 = clinopyroxenes; RT1,2 = rutiles
* indicates analyses near (i.e. 10 to 50 microns) chromite inclusions
ferric iron for chromite recalculated, based on charge balance and stoichiometry, using MINSORT (Petrakakis & Dietrich, 1985); ferric iron for garnets recalculated after Rickwood (1968); ferric iron for pyroxenes recalculated after Lindsley & Andersen (1983)

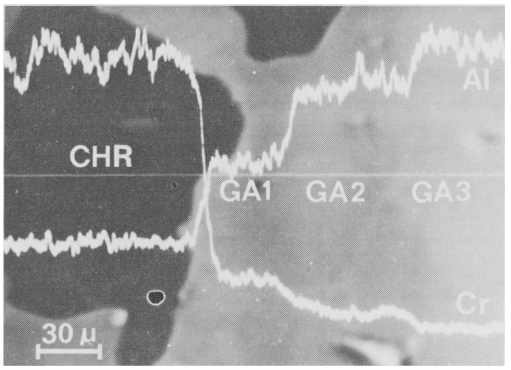

FIG. 1. Back-scattered electron picture of chromite inclusion (CHR) in uvarovite–chrome-bearing garnet (GA1–GA3) with superimposed Cr and Al X-ray profiles.

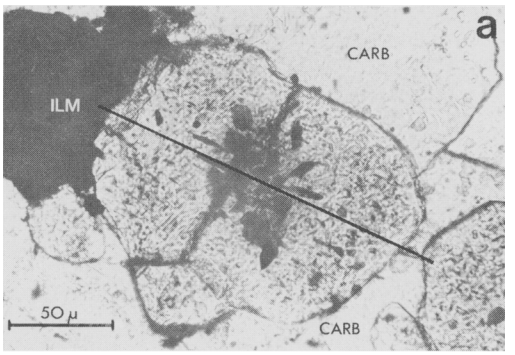

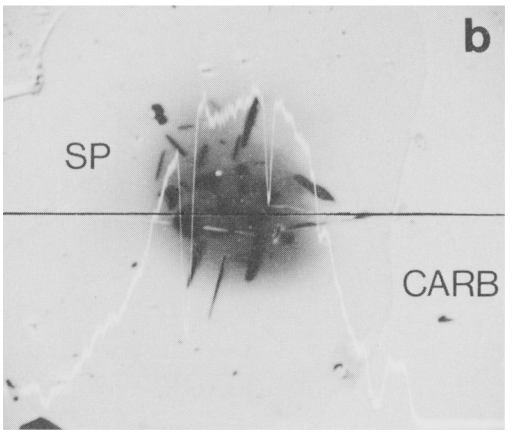

FIG. 2(*a*). Zoned chromite–chrome spinel (sample PT-166) with ilmenite-type exsolution lamellae in core (ILM = ilmenite, CARB = carbonate). The line shows the position of the analysed profile of Fig. 3. Transmitted light, parallel nicols. (*b*) Back-scattered electron picture of zoned chromite–chrome spinel (SP) with superimposed Cr X-ray profile in carbonate matrix (CARB) of sample PT-166. In core: ilmenite-type exsolution lamellae; black line indicates X-ray profile position. Magnification ×750.

decrease in Cr is balanced by an increase in Al and Fe (see Fig. 1). Based on end-member formulae the garnet changes from $Alm_{16.2}Spess_{0.7}Py_{6.8}Uv_{41.0}Gross_{29.6}And_{5.7}$ to $Alm_{31.0}Spess_{1.2}Py_{15.2}Uv_{7.1}Gross_{45.1}And_{0.5}$. Generally one would expect a significant andradite component in the garnet at the chromite rim; however, a series of recalculated garnet analyses (after Rickwood, 1968) shows insignificant amounts of Fe_2O_3. As can be seen in Table 1, the chromite associated with the garnet has no Fe_2O_3 also, which may be the reason for the garnet analyses lying in the uvarovite–grossular–almandine series, rather than in the uvarovite–grossular–andradite series. The decrease in the amount of Cr_2O_3 in the chrome-bearing garnet displays the mobility of chromium away from the chromite margin within a distance of about 100 to 150 μm.

This garnet zonation is only one example, documenting the mobility of Cr. However, there are differences in zonation patterns and a range in composition of the garnets within the domain of the chromite–garnet association. But, generally, garnet compositions near chromite (10–30 μm) always have higher Cr_2O_3 values (ranging from 5 wt. % to 13 wt. %) than the rim compositions, which give values of Cr_2O_3 from 4 wt. % to 0.02 wt. %.

Pyroxenes. As set out in Table 1, two different types of pyroxene (diopside and omphacite) are observed around the chrome garnet. The analyses near the chromite and the chrome-bearing garnet show 2–3 wt. % Cr_2O_3, whereas the amount of Cr_2O_3 is found to decrease away from the chromite–chromian garnet (0.28 to 0.03 wt. % Cr_2O_3).

Amphiboles. The amphiboles show Cr_2O_3 enrichment around the chromite–chrome garnet grains, similar to the above-mentioned garnet and pyroxenes, and a depletion in the amount of this oxide away from the chromite–chrome garnet (Table 1). The amphiboles have high alumina content of about 18 wt. %, similar to the high-alumina calcic amphiboles reported form the metabasites and meta-carbonates of Central Oetztal (Mogessie *et al.*, 1986).

Rutile. The oxide observed near the chromite–chrome-bearing garnet and the associated mafic minerals is rutile. Analyses of this oxide (Table 1) show Cr_2O_3 enrichment similar to the mafic

Table 2: Representative electronmicroprobe analyses of zoned chromite-chrome spinel and associated minerals from samples PT-166 and PT-179

	1	2	3	4	5	ILM1	ILM2	CHL1	CHL2	OL1	CHR1	OL2	CHR2
SiO_2	n.d.	n.d.	n.d.	n.d.	n.d.	-	-	27.85	33.79	42.17	n.d.	41.53	n.d.
TiO_2	0.36	0.21	0.06	-	0.02	56.88	56.59	0.06	0.03	-	0.04	-	0.24
Al_2O_3	31.91	52.41	62.13	68.72	67.65	0.11	0.04	22.86	15.39	-	61.65	0.02	37.89
Cr_2O_3	38.01	18.93	7.76	1.51	1.65	1.75	0.10	4.19	0.09	0.05	8.42	-	29.32
V_2O_5	0.62	0.33	0.21	0.08	0.19	-	0.48	n.d	n.d.	n.d.	0.30	-	0.35
Fe_2O_3	0.60	0.00	0.34	0.22	0.89	-	-	-	-	-	0.08	-	3.66
FeO	12.70	6.13	4.98	4.41	4.00	24.37	31.27	3.02	2.36	4.31	5.74	5.04	10.01
MnO	0.17	0.10	0.04	-	0.03	0.28	0.44	0.04	0.02	0.04	0.05	0.08	0.20
MgO	16.04	22.32	23.92	25.17	25.14	15.98	11.16	29.29	35.40	53.23	23.40	52.93	18.22
ZnO	0.23	0.19	0.18	-	0.17	-	0.04	n.d.	n.d.	-	0.20	0.04	0.16
Total	100.64	100.62	99.62	100.11	99.74	99.37	100.12	87.32	87.08	99.80	99.88	99.64	100.05
Oxygens	32	32	32	32	32	6	6	28	28	4	32	4	32
Si	-	-	-	-	-	-	-	5.291	6.321	1.008	-	0.999	-
Ti	0.064	0.032	0.008	-	-	1.941	1.988	0.009	0.004	-	0.008	-	0.040
Al	8.704	12.800	14.672	15.720	15.576	0.006	0.002	5.119	3.393	-	14.592	0.001	10.032
Cr	6.952	3.104	1.232	0.232	0.256	0.063	0.004	0.629	0.013	0.001	1.336	-	5.208
V	0.112	0.056	0.032	0.016	0.032	-	0.015	-	-	-	0.048	-	0.064
Fe^{3+}	0.104	0.000	0.048	0.032	0.128	-	-	-	-	-	0.016	-	0.616
Fe^{2+}	2.456	1.064	0.832	0.720	0.656	0.925	1.221	0.480	0.369	0.086	0.960	0.101	1.880
Mn	0.032	0.016	0.008	-	0.008	0.011	0.017	0.006	0.003	0.001	0.008	0.002	0.040
Mg	5.528	6.896	7.144	7.280	7.320	1.080	0.776	8.293	9.868	1.896	7.000	1.898	6.096
Zn	0.040	0.032	0.024	-	0.024	_	0.001	-	-	-	0.032	0.001	0.024
Total	23.992	24.000	24.000	24.000	24.000	4.026	4.024	19.827	19.971	2.992	24.000	3.002	24.000

analyses 1 - 4 = zoned chromite - chrome spinel (1=core, 4=rim); analysis 5 = metamorphic spinel in carbonate matrix; ILM1 = ilmenite type lamallae in zoned chromite - chrome spinel; ILM2 = ilmenite in carbonate matrix; CHL1,2 = zoned chlorite near (about 200 microns apart) chromite - chrome spinel (CHL1=core, CHL2=rim); CHR1-OL1 = olivine - chromite pair in sample PT-166; CHR2-OL2 = olivine - chromite pair in sample PT-179; ferric iron for spinels recalculated, based on charge balance and stoichiometry, using MINSORT (Petrakakis & Dietrich, 1985);

minerals given above (1.52 wt. % to 0.04 wt. % Cr_2O_3).

Type 2: chromite–spinel–carbonate

Zoned chromite–chrome spinel. This type of chromite–chrome spinel occurs in the metacarbonate sample PT-166 (mineral paragenesis: calcite ± olivine ± spinel ± phlogopite ± humite ± apatite). The chromite–chrome spinel is optically zoned with dark core and colourless rim. In the core are fine exsolution-type lamellae of ilmenite (Fig. 2*a*).

Electron microprobe profiles have been made to document the chemical zonation. As shown in Table 2, Fig. 2*b* and Fig. 3 the spinel is found to be strongly zoned with Fe and Cr-rich core (35–38 wt. % Cr_2O_3 and 9–13 wt. % FeO) and Mg and Al-rich rim (62–69 wt. % Al_2O_3 and 23–25 wt. % MgO). The chromite–chrome spinel has very low TiO_2 (<0.4 wt. %), similar to the chromite of PT-27. The zonation indicates a change from a chromite (core), chrome-spinel to a Mg-Al-spinel (rim). However, there is a variation in the range of composition from one grain to the other. The chromite–chrome spinel discussed here represents the maximum range of Cr_2O_3.

Spinel. Abundant spinel grains within the carbonate matrix and those in parageneses with zoned chromite–chrome spinels have been analysed and show no zonation, but have similar compositions to the rim of the zoned chromite-chrome spinel (Fig. 4). Almost all these spinels contain very fine, reddish needle-like inclusions or exsolution lamellae (possibly rutile) along the (111)-crystallographic direction.

Ilmenite occurs as individual grains in the carbonate matrix and as exsolution-type lamellae within the core of the zoned chromite–chrome spinel (Fig. 2*a*). The composition of the ilmenite lamellae (Table 2) shows a large amount of MgO (15.98 wt. % MgO, 53.5 mol % geikelite component) and is considered to be a picroilmenite. Even though two different textural occurrences of this mineral have been observed in sample PT-166, a large difference in chemistry has not been established. Ilmenites with similar MgO content have also been observed in several metacarbonates which do not contain chromite, but having

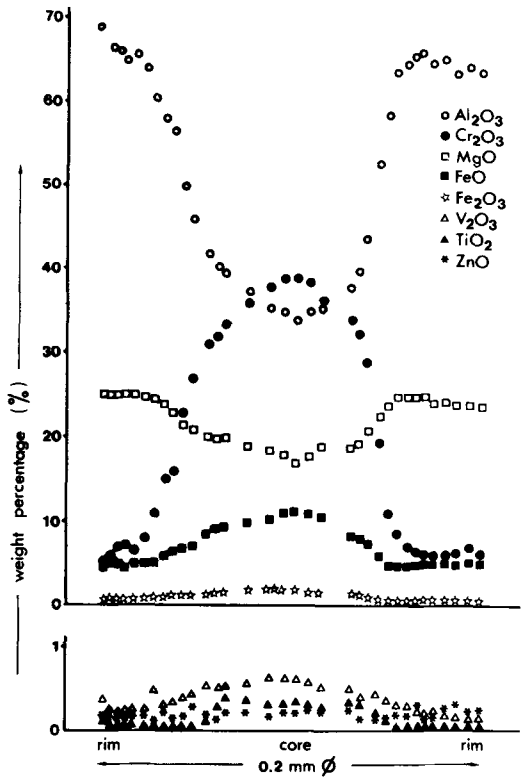

FIG. 3. Chemical profile across the zoned chromite–chrome spinel of sample PT-166 (photomicrograph see Fig. 2).

mineral parageneses like ilmenite ± carbonate ± humite ± spinel ± chlorite ± olivine.

Chlorites (about 150 to 200 μm in diameter) observed near the chromite–chrome spinel are optically zoned and contain up to 4.19 wt. % Cr_2O_3 in the core, which decreases to 0.09 wt. % at the rim (Table 2). The chlorites that are not associated with the chromite–chrome spinel domain do not contain chromium. This is a similar phenomena observed in the mafic minerals, associated with chromite and uvarovite–chrome garnet in sample PT-27.

Type 3: chromite–olivine pairs

This type of association occurs in two of the three samples (PT-166 and PT-179). The olivine–chromite pairs in PT-166 are found within the same domain as the zoned chromite–chrome spinel (type 2) discussed above.

Chromite. Analyses of chromite inclusions in olivine in both samples show zonation trends similar to the zoned chromite–chrome spinel in the carbonate matrix of sample PT-166 (Table 2), but display different ranges of compositions (39 wt. % Cr_2O_3 core, 29 wt. % rim in sample PT-179; 21 wt. % Cr_2O_3 core, 8.5 wt. % rim in sample PT-166).

Olivine. The olivine that contains the chromite–chrome spinels is homogeneous and forsteritic with max. FeO value of 5 wt. % (95–96 mol % Fo). This composition is found to be similar to the composition of the normal metamorphic olivines in the metacarbonates of Central Oetztal.

Discussion

Haggerty (1976) states that spinel, chromian spinel and related spinel species are restricted almost exclusively to mafic and ultramafic suites. A review of the chromite literature also indicates that chromites are common in kimberlites and ultrabasic rocks such as peridotites and dunites. Except for the reported occurrences of chrome minerals, including chromite, from Outokumpu in skarns and dolomitic rocks intimately associated with serpentinites (Eskola, 1933; von Knorring, 1951; von Knorring *et al.*, 1986) no chromites or chrome spinels have been so far reported from a metacarbonate unit.

The chromite of sample PT-27 is homogeneous, but has a different chemical composition [Cr/(Cr + Al) = 0.84 and Mg/(Mg + Fe^{2+}) = 0.10] to the chromite–chrome spinels of PT-166 and PT-179 (Tables 1 and 2, Fig. 4). The texture of the chromite–garnet association and the chemical composition of the chromite inclusions, suggest that the garnet has grown by a reaction between this relict magmatic chromite and carbonate, possibly by the following reaction (von Knorring, 1951):

$$\text{dolomite} + \text{chromite} + SiO_2 + H_2O = \text{tremolite} + \text{diopside} + \text{uvarovite}.$$

However, as can be seen from the chromium X-ray profile (Fig. 1), the distribution is not homogeneous and the uvarovite component of the garnet decreases away from the chromite margin. This is found to be the same for the associated mafic minerals such as amphibole and pyroxene (Table 1). Therefore, the reactions that have produced these chrome-bearing minerals seem to be complicated and suggest that they were continuous and/or discontinuous, and also that metasomatic processes might have played a major role during metamorphism.

Texturally the zoned chromite–chrome spinel of sample PT-166 occurs in a carbonate matrix. The zonation pattern (Fig. 3) is similar to the metamorphic zoned chrome spinel of Evans and

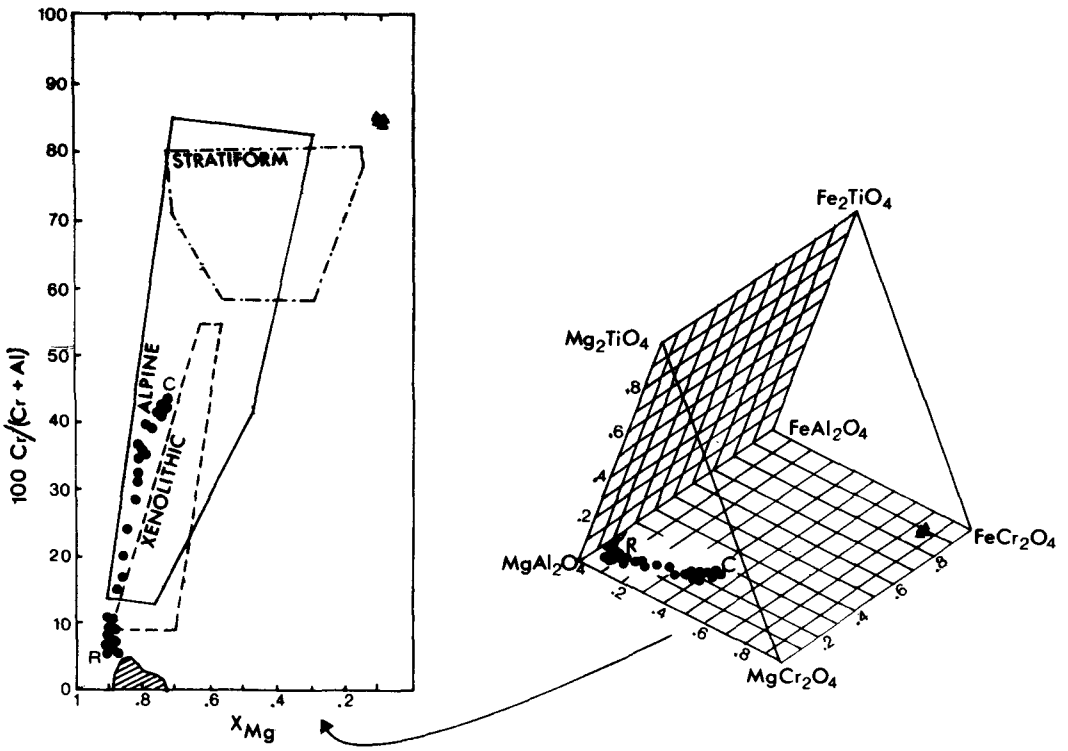

FIG. 4. Compositional plots [X_{Mg} *vs*, 100Cr/(Cr + Al) of the spinel prism] of zoned chromite–chrome spinel (sample PT-166, closed circles) from core (C) to rim (R), chromites from sample PT-27 (inclusions in uvarovite, closed triangles) and spinels from samples PT-166, PT-27, PT-179 and from other metacarbonate samples (stripped region). Fields of stratiform, alpine and xenolithic chromites are from Irvine and Findlay (1972).

Frost (1975) with differing Fe/Mg values, and different from the two magmatic chromite profiles given in Haggerty (1976).

A plot of analysed spinels from the metacarbonates, including the chrome spinels, shows a wide variation in chemistry within the $FeCr_2O_4$–$MgCr_2O_4$–$FeAl_2O_4$–$MgAl_2O_4$ base of the spinel prism (Fig. 4). The rim composition of the zoned spinel is found to be similar to the composition of the metamorphic spinels in the metacarbonates, which may suggest that the chromite–chrome spinel zonation is a result of metamorphism. This seems to be supported by the observation of Evans and Frost (1975), who stated that magnetite–chrome-magnetite–ferritchromite–low alumina chromite–high alumina chromite and Mg-Al-spinel form a continuous series that is to a large extent dependent on metamorphic grade. That rim compositions of chromites that have undergone metamorphism contain high Mg and Al is also suggested by Lipin (1984). Therefore, the rim composition of the zoned chromite–chrome spinel (Type 2, high Mg–Al) is thought to represent the metamorphic climax.

Olivine–chromite equilibrium pairs have been considered to be useful as geothermometers (Irvine, 1965). Evans and Frost (1975) investigated olivine–chromite pairs in the metamorphosed chlorite–enstatite–olivine rocks near Mt. Stuart, Washington, and metamorphosed ultramafics from the Central Alps of Switzerland and Italy, and determined a regression line on a $\ln K_D^*$ *vs.* Y_{Cr}^{SP} diagram, which they suggested corresponds to a tentative 700 °C isotherm.

Considering the textural occurrence of chromite–chrome spinel in olivine (Type 3) in the metacarbonate samples; equilibrium conditions at the metamorphic peak can be assumed. The calculated $\ln K_D^*$ values (olivine–spinel Fe–Mg partition coefficients) of the olivine–chrome spinel pairs lie on the regression line of Evans and Frost (1975). The K_D values are calculated using the rim compositions of the spinels enclosed in olivine; ($\ln K_D^* = 1.251$ and $Y_{Cr}^{SP} = 0.08$ in sample

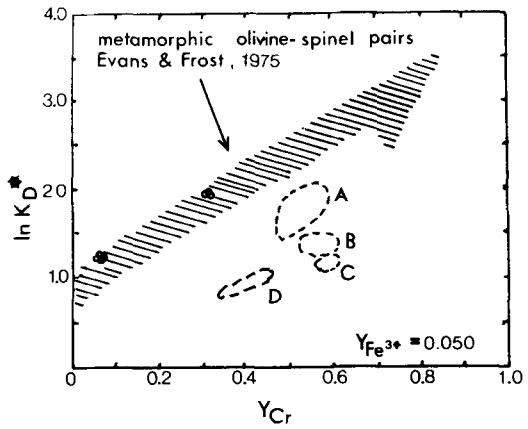

FIG. 5. Plot of $\ln K_D^*$ versus Y_{Cr}^{SP} [= Cr/(Cr + Al + Fe^{3+})] after Evans and Frost (1975) for olivine–spinel pairs in samples PT-166 and PT-179 (open circles). $\ln K_D$ has been normalized ($\ln K_D^*$) for $Y_{Fe}^{SP} = 0.050$. Field A = Stillwater H chromite layer, B = Stillwater monomineralic layers, C = Kilauea Iki pumice and D = oceanic pillow basalts.

PT-166 and $\ln K_D^* = 1.769$ and $Y_{Cr}^{SP} = 0.33$ in sample PT-179; see Fig. 5). This does not seem to be accidental, but clearly shows that the K_D is an indication of the metamorphic effects on these mineral pairs, quite different from the K_D for the magmatic olivine–chromite pairs given in Fig. 5 (A, B, C, D). The tentative 700 °C isotherm, which corresponds to the regression line (Evans and Frost, 1975), actually fits well with the high-grade amphibolite facies metamorphism of the Central Oetztal during the Hercynian time (Hoinkes *et al.*, 1982).

The magnesium analogue of ilmenite is a characteristic accessory mineral in rocks with high Mg/Fe ratios. It is found in serpentinized ultramafic rocks (Trommsdorf and Evans, 1980), in kimberlites (Meyer, 1977; Mitchell, 1977), in carbonatites (Mitchell, 1978) and in impure magnesian limestones (Murdoch and Fahey, 1949; Wise, 1959; Gieré, 1984).

The MgO value of the ilmenite lamellae within the zoned chromite–chrome spinel core and the individual ilmenite grains in the carbonate matrix have been found to be of almost the same composition. The fact that these MgO-rich ilmenites occur in most of the metacarbonate mineral parageneses of Central Oetztal implies that the ilmenite exsolution lamellae within the chromite core may have resulted from metamorphism.

Genetic considerations

Based on field relations, the metacarbonate unit is found to occur as small lenses or layers always at the edges of the amphibolite mass, bounded by metabasites and granitic gneisses. The fact that the whole region has been subjected to polymetamorphism of variable grade (Hoinkes *et al.*, 1982) makes it difficult to suggest how chromite was introduced into the carbonate units. However, the mineral parageneses in the metacarbonates, the metamorphic zonation of the chromite–chrome spinel, and the K_D values of the olivine–chrome spinel pairs are found to be representative of the Hercynian amphibolite metamorphism of this part of the Eastern Alps (Purtscheller and Sassi, 1975; Purtscheller and Tessadri, 1985; Mogessie *et al.*, 1986). Therefore chromium (certainly bounded in magmatic chromite, as type 1 shows) must have been introduced, or was part of the carbonate before the Hercynian amphibolite facies metamorphism took place.

Acknowledgements

We thank E. Mersdorf (University of Innsbruck) for helpful guidance during electron microprobe work. We are grateful to an unknown reviewer for a critical review of the original manuscript. This work was supported by the Fonds zur Förderung der wissenschaftlichen Forschung (P4843 and P5541).

References

Bence, A. E. and Albee, A. L. (1968) *J. Geol.* **76**, 382–403.

Eskola, P. (1933) *Bull. Comm. Geol. Finlande* **103**, 26–44.

Evans, B. W. and Frost, B. R. (1975) *Geochim. Cosmochim. Acta* **39**, 959–72.

Gieré, R. (1984) Diplomarbeit ETH Zürich.

Haggerty, S. E. (1976) In *Oxide Minerals* (D. H. Rumble III, ed.). Mineral. Soc. Am. Short Course Notes **3**, 101–300.

Hoinkes, G., Purtscheller, F. and Tessadri, R. (1982) *Geol. Palaeont. Mitt. Innsbruck* **12**, 95–113.

Irvine, T. N. (1965) *Can. J. Earth Sci. Rev.* **13**, 251–81.

——and Findlay, T. C. (1972) *Publ. Earth Phys. Branch. Dept Energ. Mines Resour.* **42**, 97–140.

Lindsley, D. H. and Andersen, D. J. (1983) *J. Geophys. Res.* **88**, suppl. A, 887–906.

Lipin, B. R. (1984) *Am. J. Sci.* **284**, 507–29.

Meyer, H. A. O. (1977) *Earth Sci. Rev.* **13**, 251–81.

Mitchell, R. H. (1977) *Lithos* **10**, 29–37.

——(1978) *Am. Mineral.* **63**, 544–7.

Mogessie, A. and Purtscheller, F. (1986) *Jahrb. Geol. B.-A.* **129**, 69–91.

————and Tessadri, R. (1985) *Chem. Geol.* **51**, 103–13.

————————(1986) *Neues Jahrb. Mineral., Abh.* **154**, 21–39.

Murdoch, J. and Fahey, J. J. (1949) *Am. Mineral.* **34**, 835–8.

Petrakakis, K. and Dietrich, H. (1985) *Neues Jahrb. Mineral., Mh.* 379–84.
Purtscheller, F. and Rammlmair, D. (1982) *Tschermaks Mineral. Petrogr. Mitt.* **29**, 205–21.
——and Sassi, F. P. (1975) Ibid. **22**, 175–99.
——and Tessadri, R. (1985) *Mineral Mag.* **49**, 523–9.
Rickwood, P. C. (1968) *Contrib. Mineral. Petrol.* **18**, 175–98.
Trommsdorf, V. and Evans, B. W. (1980) Ibid. **72**, 229–42.
von Knorring, O. (1951) *Mineral. Mag.* **29**, 594–601.
——Condliffe, E. and Tong, Y. L. (1986) *Bull. Geol. Soc. Finland* **58**, 277–92.
Wise, W. S. (1959) *Am. Mineral.* **44**, 879–82.

[*Manuscript received 13 February 1987: revised 22 June 1987*]